Journal Name

ARTICLE

Anti-inflammatory Diterpene Dimers from the Root Barks of *Aphanamixis grandifolia*

Hong-Jian Zhang, Yang-Mei Zhang, Jian-Guang Luo, Jun Luo* and Ling-Yi Kong*

A total of 14 new diterpene dimers, aphanamenes C−P (**1−14**) with four known homologous compounds were isolated from the root barks of *Aphanamixis grandifolia* Bl.. The structures of these compounds were elucidated by spectroscopic analyses, and their absolute configurations were determined using the CD exciton chirality method. In addition, all the compounds exhibited significant inhibition of lipopolysaccharide-induced nitric oxide production in RAW264.7 macrophages, with IC_{50} values between 7.75−38.23 μM.

Introduction

The species *Aphanamixis grandifolia* (Meliaceae) is a wild timber tree mainly distributed in the tropical areas of the south of China, Indo China Peninsula, Malaysia and Republic Indonesia.[1] The roots and leaves are utilized to relieve rheumatoid joint pain and numbness of limbs in some regions of China.[2] Previous phytochemical studies on the genus *Aphanamixis*, indicated that they are a rich resource of structurally diverse and highly oxygenated triterpenoids and limonoids.[3–9] Recently, the search for bioactive compounds from this species lead to the discovery of one type of acyclic diterpene dimer with a unique carbon skeleton, which showed significant inhibition of NO production on lipopolysaccharide (LPS)-induced RAW264.7 macrophages.[10] This discovery attracted a broad range of interests by chemists in the field of organic chemistry.[11, 12] As an ongoing program to explore structural diversity and to screen bioactive natural products, fourteen new diterpene dimers, aphanamenes C−P (**1−14**) together with four known homologous compounds aphadilactones A−D (**15−18**)[11] (Fig. 1) were isolated from the root barks of *A. grandifolia*. The inhibitory effects of the isolated compounds on NO production in LPS-induced RAW264.7 macrophages were evaluated. Herein, we describe the isolation and structural elucidation of the new compounds as well as the assessment of their anti-inflammatory effects.

Results and discussion

Aphanamene C (**1**) was obtained as a colourless gum. The molecular formula $C_{40}H_{54}O_8$ with 14 degrees of unsaturation, was determined by HRESIMS data at *m/z*: 685.3712 [M + Na]$^+$ (calcd 685.3711). Its IR spectrum displayed absorption bands at 1696 cm^{-1} and 1613 cm^{-1}, indicating the presence of carbonyl and double bond groups, respectively. Overall analysis of the NMR data (Tables 1 and 2) further implied that **1** was a diterpene dimer which was similar to aphanamene B and aphadilactone A, which was also formed by two diterpene molecules via a Diels-Alder reaction.[10,11] Four proton-bearing

structural fragments, corresponding to H-4−H-6, H-8−H-18′, H-4′−H-6′ and H-8′−H-10′ (Fig. 2), that were observed by analysis of the ^{1}H-^{1}H COSY spectra. The HMBC spectrum of **1** (Fig. 2) exhibited the correlations of H-11/C-18′ and H-10′/C-13 demonstrated that units I and II should be linked via two C-C single bonds (between C-18 and C-18′, C-13 and C-11′) arising from the Diels-Alder cycloaddition, and a cyclohexene ring with Pro-dimethylene was formed by a head-tail dimerization in the same way as aphadilactone A[11] (see ESI Scheme S1†). An α, β-unsaturated carboxylic acid fragment was confirmed by HMBC of H-2/C-1, H-5/C-3, H-16/C-4 (Fig. 2 unit I) of **1**, which was the main difference between **1** and aphadilactone A. Establishment of the $\Delta^{6(7)}$ and $\Delta^{6'(7')}$ double bonds, which were
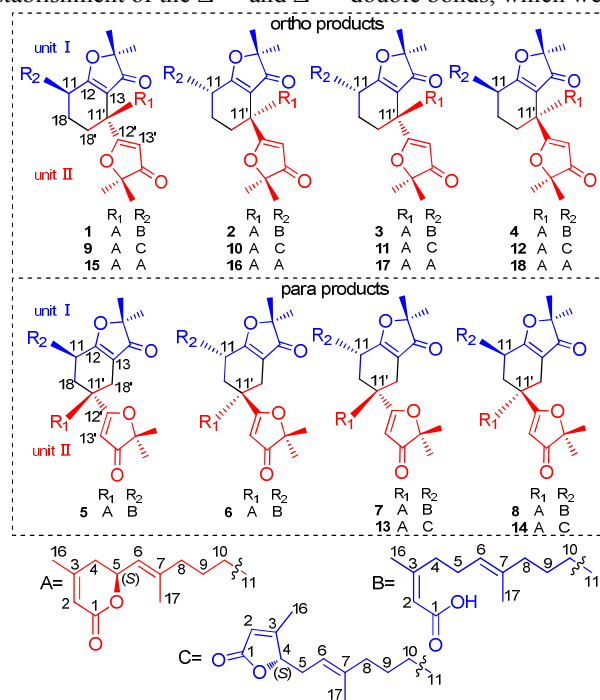

Fig. 1 Structures of compounds **1−18**.

confirmed by the HMBCs of H-5/C-6, C-7 and H-5′/C-6′, C-7′, respectively (Fig. 2). The planar structure of **1** was thus established (Fig. 1).

In the ROESY spectrum of **1** (Fig. 3), the key correlations of H-11 with H-18′α and H-10a with H-18β showed that they adopted 1, 3-diaxial positions in the half-chair cyclohexene ring, and H-11 was arbitrarily fixed as α-oriented. Consequently, the long chain at C-11′ of **1** was indirectly assigned as β-orientation by the key correlation of H-13′ with H-18′α. Thus, the two wings at C-11 and C-11′ incorporating α, β-unsaturated carboxylic acid and a lactone ring at C-11 and C-11′ of the cyclohexene ring in **1** were definitely assigned as *cis*-oriented. Thus, the structure of **1** was determined as shown (Fig. 1).

The HRESIMS, UV, IR, ^{1}H and ^{13}C NMR (Tables 1 and 2) data for aphanamenes D−F (**2−4**) showed great similarities to those of **1**, and the obvious variations between them were the ^{1}H
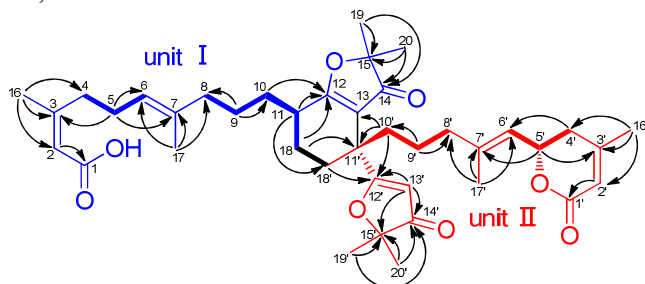
NMR resonances around the cyclohexene ring (e. g. H-11 and H-13′). Comprehensive analysis of spectra of **2−4** (see ESI S9−S24†), especially of the 2D NMR spectra, verified that **2−4** possess the same planar structure as **1** (Fig. 1), and they were stereoisomers at C-11 and C-11′. The key ROESY correlations of H-10a with H-18α, H-18′β with H-11 and H-13′ suggested that the relative configurations of the wings at C-11 and C-11′ of **2** both had α-orientation, which were contrary to those of **1** (Fig. 3). In a similar fashion, the two wings at C-11 and C- 11′ in **3** and **4** were determined to be *trans*-oriented in the
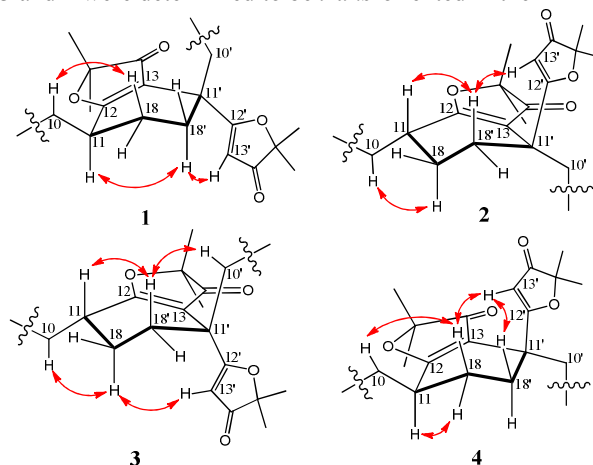

Fig. 3 Key ROESY correlations (↔) of **1−4**.

Fig. 2 Key ^{1}H-^{1}H COSY (▬) and HMBC (H→C) correlations of **1**.

Table 1 ^{1}H NMR Spectroscopic Data (500 MHz, CDCl$_3$) for Compounds **1**, **3**, **5** and **7** (δ_H in ppm, J in Hz)

no.	1	3	5	7	no.	1	3	5	7
2	5.67, s	5.66, s	5.69, s	5.68, s	2′	5.83, s	5.81, s	5.81, s	5.81, s
					4′a	2.38, dd	2.37, dd	2.37, dd	2.37, dd
4	2.64, t (7.5)	2.65, m^a	2.65, t (8.0)	2.70, m^a		(11.0, 18.0)	(11.5, 17.5)	(11.0, 18.0)	(11.5, 17.5)
					4′b	2.21, dd	2.21, dd	2.24, dd	2.21, dd
5	2.16, dd	2.15, dd	2.18, dd	2.16, dd		(4.0, 18.0)	(4.0, 18.0)	(4.0, 18.0)	(3.5, 18.0)
	(7.5, 14.5)	(7.5, 15.0)	(7.5, 15.0)	(6.5, 14.0)	5′	5.12, m^a	5.10, m^a	5.10, m^a	5.09, m^a
6	5.12, m^a	5.10, m^a	5.18, t (7.0)	5.14, t (6.5)^a	6′	5.35, d (8.5)	5.31, d (8.5)	5.30, d (8.5)	5.30, d (8.5)
8	1.95, m^a	2.03, m^a	2.01, m^a	1.95, m^a	8′	2.08, dd	1.94, m^a	2.01, m^a	2.08, dd
						(6.0, 14.0)			(6.0, 14.0)
9	1.87, 1.56, m^a	1.90, m^a	1.90, m^a	1.87, 1.56, m^a	9′	1.74, 1.81, m^a	1.94, m^a	1.90, m^a	1.74, 1.81, m^a
10a	1.47, m^a	1.43, m^a	1.70, m^a	1.47, m^a	10′a	1.89, m^a	1.83, m^a	2.05, m^a	1.89, m^a
10b	1.73, m^a	1.65, m^a	1.45, m^a	1.75, m^a	10′b	1.77, m^a	2.07, m^a	1.78, m^a	1.77, m^a
11	2.50, m	2.55, m	2.49, m	2.57, m	13′	5.31, s	5.23, s	5.24, s	5.32, s
16	1.90, s	1.90, s	1.92, s	1.90, s	16′	1.99, s	1.98, s	1.98, s	1.98, s
17	1.56, s	1.54, s	1.61, s	1.57, s	17′	1.72, s	1.69, s	1.64, s	1.67, s
18α	1.82, m^a	1.40, m^a	1.72, m^a	1.82, m^a	18′α	1.82, m^a	1.68, m^a	1.75, m^a	1.72, m^a
18β	1.72, m^a	1.46, m^a	1.78, m^a	1.95, m^a	18′β	1.95, m^a	1.84, m^a	1.87, m^a	1.82, m^a
19	1.36, s	1.36, s	1.35, s	1.36, s	19′	1.35, s	1.35, s	1.35, s	1.38, s
20	1.35, s	1.36, s	1.35, s	1.35, s	20′	1.31, s	1.33, s	1.32, s	1.36, s

^{a} Overlapping signal

Table 2 ^{13}C NMR Spectroscopic Data (125 MHz, CDCl$_3$) for Compounds **1**, **3**, **5** and **7**

no.	1	3	5	7	no.	1	3	5	7
1	169.2	169.7	170.1	168.0	1′	165.1	165.0	165.2	165.1
2	115.8	115.6	115.6	115.6	2′	116.7	116.6	116.6	116.6
3	161.9	162.4	162.8	161.8	3′	156.7	156.7	157.0	156.8
4	33.3	33.3	33.4	33.3	4'	35.0	35.0	35.0	35.0
5	26.5	26.5	26.6	26.5	5′	74.0	74.0	74.1	74.1
6	123.8	123.5	123.8	123.9	6′	122.4	122.3	122.4	121.9
7	135.2	135.4	135.3	134.9	7′	141.9	141.9	141.9	142.1
8	39.7	39.2	39.2	39.3	8′	39.1	39.6	39.6	39.3
9	25.0	25.0	25.5	24.9	9′	29.6	30.3	25.5	26.5
10	31.2	30.4	31.3	33.3	10′	29.0	34.4	34.4	34.0
11	35.4	36.4	35.2	36.5	11′	41.6	42.0	41.7	42.0
12	189.6	189.6	190.3	190.1	12′	194.7	195.1	194.6	195.2
13	111.2	111.4	110.5	111.1	13′	101.3	101.7	101.4	102.1
14	204.0	204.2	204.0	204.2	14′	207.5	207.2	207.2	207.8
15	87.6	87.7	87.5	87.7	15′	88.7	88.9	88.8	89.2
16	25.3	25.4	25.4	25.1	16′	22.7	23.1	23.0	22.8
17	15.6	15.6	15.7	15.7	17′	16.5	16.5	16.3	16.8
18	23.8	24.0	23.5	23.1	18′	35.0	35.0	28.3	24.0
19	22.7	22.8	22.8	22.8	19′	22.7	22.7	22.7	22.7
20	22.8	22.7	22.8	22.8	20′	22.6	22.7	22.7	22.3

half-chair cyclohexene ring, and adopted as α/β and β/α orientations, respectively (Fig. 3). Due to the effect of shielded coplanar of α, β-unsaturated γ-lactone moiety, the resonance of H-11 (δ_H 2.49−2.50) in **1** and **2** transfer to up-field compared with H-11 (δ_H 2.55−2.58) in **3** and **4**. In summary, the structures of **1**−**4** were finally determined, and the two wings at C-11 and C-11′ were assigned as *cis*-oriented for **1** and **2** and *trans*-oriented for **3** and **4**.

Aphanamene G (**5**) was obtained also as a colourless gum, and its molecular formula was assigned to be the same as that of **1** (C$_{40}$H$_{54}$O$_8$) by HRESIMS (*m/z*: 685.3704 [M + Na]$^+$, calcd for C$_{40}$H$_{54}$NaO$_8$, 685.3711). The ^{1}H and ^{13}C NMR spectra of **5** were almost the same as those of **1**, and the subtle differences between them were the H-18 (δ_H 1.72, 1.78), H-18′ (δ_H 1.75, 1.87) and H-13′ (δ_H 5.24) in **5**, in contrast to H-18 (δ_H 1.72, 1.82), H-18′ (δ_H 1.82, 1.95) and H-13′ (δ_H 5.31) in **1**. The key HMBC correlations of H-18/C-12′, H-18′/C-12 and H-11/C-11′ (see ESI S29†) implied that units Ⅰ and Ⅱ should be linked via C-18 and C-11′, C-13 and C-18′. A cyclohexene ring with Meta-dimethylene was fixed by head-head dimerization like that of aphanamene B[10], and the planar structure of **5** was determined (Fig.1). The key ROESY correlations (see ESI S30†) of H-18α with H-13′ and H-11 revealed that the cyclohexene moiety adopted a half-chair conformation. Furthermore, the observation of correlations of H-18β with H-10a and H-10′a indicated that the two wings at C-11 and C-11′ in **5** were *cis*-oriented, and they were arbitrarily assigned as β-configuration. Thus, the structure of **5** was established (Fig. 1).

The same molecular formula (C$_{40}$H$_{54}$O$_8$) was determined from HRESIMS and similar NMR data (see ESI S33-S44†) implied

that aphanamenes G−J (**5**−**8**) were stereoisomers with different configurations at C-11 and C-11′ as those of compounds **1**−**4** (Fig. 1). In a similar fashion, the key ROESY correlations (see ESI S34, S40 and S44†) of H-18β with H-13′ and H-11 of **6**, H-18α with H-10a and H-13′ of **7** and H-18β with H-13′ and H-10a of **8** helped us to resolve the problem of relative configurations, which means that the two wings at C-11 and C-11′ were assigned as *cis*-oriented in **5** and **6**, and *trans*-oriented in **7** and **8**. The resonance of H-11 in **5**−**8** (Table 1) further confirmed the above assignments.

Aphanamenes K−N (**9**−**12**) were colourless gums, all of them have the same molecular formula of C$_{40}$H$_{52}$O$_8$ as determined by the HRESIMS, respectively. Comprehensive analysis of the NMR data of **9**−**12** (see ESI S46-64†), their planar structures were established by the key HMBC correlations as the two units were linked between C-18 and C-18′, C-13 and C-11′ as the same connection as those of **1**−**4** (Fig. 1). 2 mass unit less than that of **1** and the down-field ^{1}H and ^{13}C NMR resonance (δ_H 4.85-4.88, δ_C 84.2-87.5) in **9**−**12** suggested that, an α, β-unsaturated carboxylic acid fragment in **1** was substituted by an α, β-unsaturated γ-lactone in **9**−**12**. The HMBC correlations of H-4 (δ_H 4.85) with C-1 (δ_C 172.9), C-2 (δ_C 117.2), C-3 (δ_C 168.0) and of Me-16 (δ_H 2.03) with C-4 (δ_C 84.2) (see ESI S49†) indicated that an α, β-unsaturated γ-lactone formed between COOH-1 and C-4 in unit Ⅰ of aphanamene K (**9**). Similarly, the relative configurations at C-11 and C-11′ of **9**−**12** were assigned as depicted by the key ROESY correlations of **9** (H-18′β with H-10′a, and H-18′α with H-11 and H-13′), **10** (H-18′β with H-11 and H-13′), **11** (H-18′β with H-11 and H-10′a) and

12 (H-18β with H-10a and H-13′) (see ESI S50, S54, S60 and S64†) suggested that the two wings were *cis*-oriented in **9** and **10** and *trans*-oriented in **11** and **12**.

Depending on their HRESIMS and NMR data, **13** and **14** were very similar to the **9−12**. Extensive interpretation of the NMR data (see ESI S66-S74†) showed that **13** possessed the same units as those of **9−12**, but had a different linkage via two C-C single bonds (between C-18 and C-11′, C-13 and C-18′). The same planar structure of **13** and **14** was confirmed by comparing their NMR spectra. The relative configurations of **13** and **14** (Fig. 1) were attributed by the key ROESY correlations of H-18α with H-11 and H-13′, H-18β with H-11 and H-13′ (see ESI S70 and S74†), which means that the two wings at C-11 and C-11′ in **13** and **14** were definitely assigned as *trans*-oriented. Accordingly, the structure of **13** and **14** were fixed (Fig. 1) and named aphanamenes O and P.
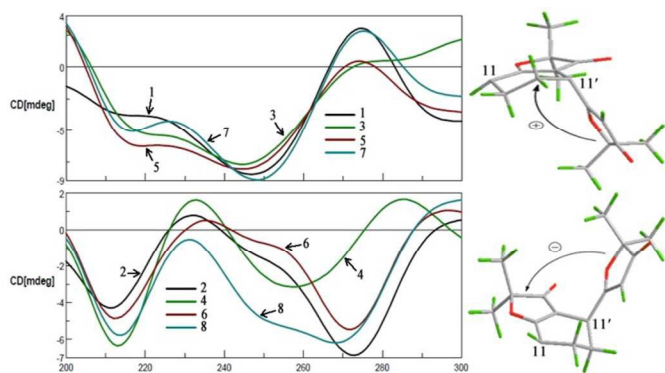

Fig. 4 CD spectra of **1-8**.

The CD exciton chirality method was used to establish the absolute configurations of C-11 and C-11′ about these molecules (Fig. 4).[11] Two chromophores of the 2, 2-dimethylfuran-3(2*H*)-one moieties[13] were considered as the main exciton chromophores in **1-14**. The clear first negative Cotton effect (CE) (λ = 247 nm) and the second positive CE (λ = 275 nm) of **1** showed a positive helicity between two chromophores, thus establishing 11*R*/11′*R* configuration for compound **1**. Consequently, the opposite CD curves (positive CE at 232 nm, negative CE at 273 nm) of **2** indicated that **2** has 11*S*/11′*S* configuration. In the same way, the absolute configurations at C-11 and C-11′ of **3** and **4** were assigned 11*S*/11′*R* and 11*R*/11′*S*. Due to the observation of the same chromophores in **5−8** (Fig. 4), the absolute configurations at C-11 and C-11′ were established as 11*R*/11′*R*, 11*S*/11′*S*, 11*S*/11′*R* and 11*R*/11′*S*. The absolute configurations of **9−14** were also determined using their typical CD spectra combined with their relative configurations (see ESI Fig. S1†). Additionally, the CD spectra of **1−14** exhibited negative Cotton effects near 210 and 250 nm, which indicated that the absolute configurations of chiral carbon (C-4 and C-5′) in **1−14** were all *S*-configurations.[14,15]

Bioassays for NO inhibitory and cytotoxic activity

The anti-inflammatory activities of the isolated compounds were evaluated by examining their ability to inhibit NO production in vitro in LPS-induced RAW264.7 macrophages. Cell viability was examined by the MTT assay, and none of the test compounds exhibited cytotoxicity at 50 μM. As shown in Table 3, compounds exhibited significant inhibitory activity with IC$_{50}$ values between 7.75−38.23 μM.

Table 3 Inhibitory Effects of **1−18** on NO Production (IC$_{50}$)

| No.	Anti-inflammatory activity (μM)	No.	Anti-inflammatory activity (μM)
1	11.87	**11**	16.35
2	10.26	**12**	16.07
3	10.74	**13**	18.63
4	19.31	**14**	18.56
5	7.75	**15**	25.34
6	11.65	**16**	37.19
7	8.86	**17**	30.54
8	13.67	**18**	38.23
9	17.58	LPS	−
10	17.25	Positive control*	40.45

*N-monomethyl-L-arginine

Conclusions

In summary, a total of 14 new diterpene dimers belong to two types of skeletons classified by the kind of central cyclohexene rings, aphanamenes C−P (**1−14**) with 4 know homologous compounds aphadilactones A−D (**15−18**), which were isolated from the root barks of *A. grandifolia*. In a plausible biosynthetic pathway, the compounds nemoralisins B, C, E and J [6, 14, 15] were considered as precursors (see ESI Scheme S1 †). On the catalysis of enzyme or UV, a new cyclohexene ring was formed between the $\Delta^{11(18),12(13)}$ and $\Delta^{11′(18′)}$ of these precursors. The precursors could undergo two kinds of connection head-head (C-13 to C-18′ and C-18 to C-11′) (Scheme 1) or head-tail (C-18 to C-18′ and C-13 to C-11′) via Diels-Alder reaction, and lead to produce a pair of epimers at C-11′ (ortho/para products). All the compounds were finally produced via a typical 1, 3-hydrogen migration which resulting in the stereoisomers at C-11 (Scheme 1). Attention to the structure-activity relationship suggested that the anti-inflammatory activity might be dependent on the polarity of the compounds. When increasing the polarity of compounds will increase the activity (Table 3). The results shed light on the discovery of new anti-inflammatory agents.

Experimental section

General experiment procedures

Optical rotations were determined with a JASCO P-1020 polarimeter. UV spectra were performed on a Shimadzu UV-2450 spectrophotometer. CD spectrum was measured on a JASCO 810 spectropolarimeter. IR spectra were recorded in KBr-disc on a Bruker Tensor 27 spectrometer. 1D and 2D NMR spectra were acquired on a Bruker AV-500 NMR instrument at 500 MHz (^{1}H) and 125 MHz (^{13}C) in CDCl$_3$. ESI and HRESI mass spectra were obtained on an Agilent 1100 series LC-MSD-Trap-SL mass analyzer and an Agilent 6520B Q-TOF mass instrument, respectively. Column chromatography (CC) was done with Silica gel (Qingdao marine Chemical Co., Ltd., China), ODS (40–63μm, FuJi, Japan). Preparative HPLC was carried out using a Shimadzu LC-8A equipped with a Shim-pack RP-C18 column (20×200 mm, i.d.) with a flow rate of 10.0 mL/min and a chiral AD-H column (10×250 mm, 5μm, Daicel Chemical Industries, Ltd.) were used for the semipreparative HPLC analysis, detected by a binary channel UV detector.
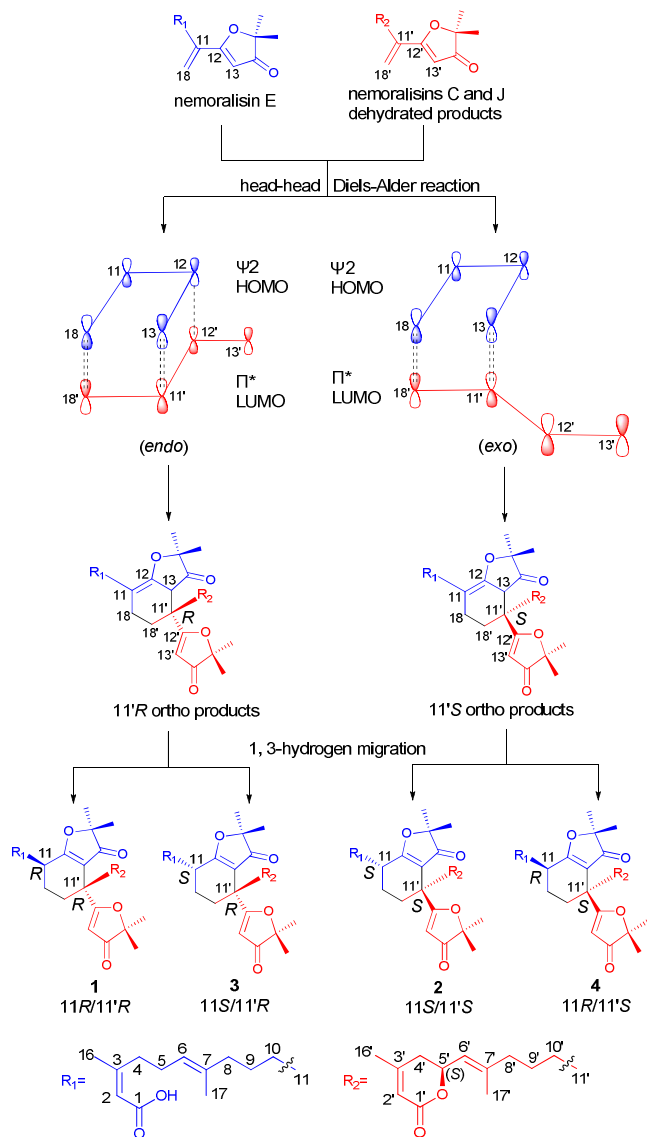
Scheme 1 Plausible biosynthetic pathway of stereoisomers (**1-4**).

Plant material

The root barks of *Aphanamixis grandifolia* Bl. were collected from Yunnan Province of China in October 2012, and were authenticated by Professor Min−Jian Qin, Department of Medicinal Plants, China Pharmaceutical University. A voucher specimen (No. 121026) is deposited in the Department of Natural Medicinal Chemistry, China Pharmaceutical University.

Extraction and isolation

The air-dried root barks of *A. grandifolia* (3.1kg) were exhaustively extracted with 95% EtOH (3×4h). The EtOH extract was concentrated under reduced pressure. The crude extract (320g) was suspended in water and successively partitioned with Chloroform (CHCl₃). The CHCl₃ fraction yielded 75g after removal of the fatty components by extracting with petroleum ether (PE). The CHCl₃ fraction was performed on a silica gel column using a gradient of CH_2Cl_2–MeOH (100:1−2:1) to afford four fractions (Fr. C1−4) by TLC analysis. Fr. C3 (20 g) was eluted in a gradient system on CC over silica gel with petroleum ether–acetone (7:1, 5:1, 2:1), to yield five

sub-fractions (Fr. C3.1–3.5). Fr. C3.3 was then applied onto an ODS column using a stepwise of MeOH–H₂O (50:50 to 90:10), to give five sub-fractions (Fr. C3.3.1–3.3.5). Fr. C3.3.2 was further purified on ODS column with CH₃CN–H₂O (65:35), to yield four subfractions (Fr. C3.3.2.1–3.3.2.4). Fr. C3.3.2.4 was then further purified by preparative HPLC with CH₃OH–H₂O (65:35, 10 mL/min) to obtain peaks A−D. Peak A was thus subjected to a further purification process by semipreparative HPLC using a chiral AD-H column with n-hexane/isopropanol/ethanol (70:10:20, v/v/v, 2 mL/min) as the mobile phase to yield compounds **1** (14mg) and **2** (16mg). In the same way, peak B afforded **3** (16mg) and **4** (17mg); peak C afforded **5** (20mg) and **6** (22mg); peak D afforded **7** (6mg) and **8** (8mg) Fr. C3.3.2.2 was then further purified on preparative HPLC with CH₃OH–H₂O (62:38, 10 mL/min) to obtain peak E. Also using the chiral column with the same mobile phase, peak E to yielded **14** (4.2mg) and **13** (4.3mg).

Fr. C3.4 was then applied onto an ODS column using a stepwise of MeOH–H₂O (50:50 to 90:10), to give five subfractions (Fr. C3.4.1–3.4.5). Fr. C3.4.2 was further purified on ODS column with a step gradient of MeOH–H₂O (50:50 to 90:10), to give four subfractions (Fr. C3.4.2.1–3.4.2.4). Fr. C3.4.2.3 was then repeatedly purified on preparative HPLC with CH₃OH–H₂O (72:28, 10 mL/min) and CH₃CN–H₂O (65:35, 10 mL/min) to obtain peaks F−I. In the same way as Fr.C3.3.2.4, the pesks were separate using the chiral column to yield **15** (9.7mg) and **16** (13.5mg), **17** (7.7mg) and **18** (9.7mg), **9** (8.0mg) and **10** (7.8mg), **11** (8.0mg) and **12** (13.4mg).

Aphanamene C (1). Colourless gum; $[\alpha]^{25}_D$ −19.6 (*c* 0.10, MeOH); UV (MeOH) λ_{max} (log ε) 208 (2.44), 265 (1.76) nm; IR (KBr) ν_{max} 3444, 2855, 1696, 1613, 1383, 1249 cm⁻¹; for ¹H and ¹³C NMR data, see Tables 1 and 2; ESIMS (positive) *m/z* 663.6 [M+H]⁺; HRESIMS *m/z* 685.3708 [M+Na]⁺ (calcd for C₄₀H₅₂NaO₈, 685.3711).

Aphanamene D (2). Colourless gum; $[\alpha]^{25}_D$ +12.6 (*c* 0.10, MeOH); UV (MeOH) λ_{max} (log ε) 214 (3.02), 265 (1.57) nm; IR (KBr) ν_{max} 3451, 2856, 1696, 1613, 1383, 1249 cm⁻¹; for ¹H NMR data, see Table 1; ESIMS (positive) *m/z* 663.6 [M+H]⁺; HRESIMS *m/z* 685.3708 [M+Na]⁺ (calcd for C₄₀H₅₂NaO₈, 685.3711).

Aphanamene E (3). Colourless gum; $[\alpha]^{25}_D$ −32.6 (*c* 0.16, MeOH); UV (MeOH) λ_{max} (log ε) 200 (3.07), 265 (1.51) nm; IR (KBr) ν_{max} 3450, 2856, 1696, 1612, 1383, 1248 cm⁻¹; for ¹H and ¹³C NMR data, see Tables 1 and 2; ESIMS (positive) *m/z* 663.6 [M+H]⁺; HRESIMS *m/z* 685.3709 [M+Na]⁺ (calcd for C₄₀H₅₄NaO₈, 685.3711).

Aphanamene F (4). Colourless gum; $[\alpha]^{25}_D$ +17.0 (*c* 0.10, MeOH); UV (MeOH) λ_{max} (log ε) 200 (2.82), 265 (1.19) nm; IR (KBr) ν_{max} 3450, 2856, 1696, 1612, 1383, 1249 cm⁻¹; for ¹H NMR data, see Table 1; ESIMS (positive) *m/z* 663.6 [M+H]⁺; HRESIMS *m/z* 685.3709 [M+Na]⁺ (calcd for C₄₀H₅₄NaO₈, 685.3711).

Aphanamene G (5). Colourless gum; $[\alpha]^{25}_D$ −19.8 (*c* 0.10, MeOH); UV (MeOH) λ_{max} (log ε) 198 (2.21), 264 (0.19) nm; IR (KBr) ν_{max} 3450, 2856, 1695, 1612, 1383, 1249 cm⁻¹; for ¹H and ¹³C NMR data, see Tables 1 and 2; ESIMS (positive) *m/z* 663.6 [M+H]⁺; HRESIMS *m/z* 685.3704 [M+Na]⁺ (calcd for C₄₀H₅₄NaO₈, 685.3711).

Aphanamene H (6). Colourless gum; $[\alpha]^{25}_D$ +16.8 (*c* 0.10, MeOH); UV (MeOH) λ_{max} (log ε) 199 (2.34), 265 (0.43) nm; IR (KBr) ν_{max} 3442, 2856, 1696, 1612, 1383, 1249 cm⁻¹; for ¹H NMR data, see Table 1; ESIMS (positive) *m/z* 663.6 [M+H]⁺; HRESIMS *m/z* 685.3704 [M+Na]⁺ (calcd for C₄₀H₅₄NaO₈, 685.3711).

Aphanamene I (7). Colourless gum; $[\alpha]^{25}_D$ +15.4 (*c* 0.10, MeOH); UV (MeOH) λ_{max} (log ε) 202 (3.56), 265 (1.76) nm; IR (KBr) v_{max} 3450, 2858, 1697, 1613, 1385, 1251 cm^{-1}; for ^{1}H and ^{13}C NMR data, see Tables 1 and 2; ESIMS (positive) *m/z* 663.5 [M+H]$^+$; HRESIMS *m/z* 685.3705 [M+Na]$^+$ (calcd for C$_{40}$H$_{54}$NaO$_8$, 685.3711).

Aphanamene J (8). Colourless gum; $[\alpha]^{25}_D$ −17.3 (*c* 0.10, MeOH); UV (MeOH) λ_{max} (log ε) 204 (2.53), 265 (1.26) nm; IR (KBr) v_{max} 3447, 2856, 1696, 1613, 1383, 1249 cm^{-1}; for ^{1}H NMR data, see Table 1; ESIMS (positive) *m/z* 663.5 [M+H]$^+$; HRESIMS *m/z* 685.3705 [M+Na]$^+$ (calcd for C$_{40}$H$_{54}$NaO$_8$, 685.3711).

Aphanamene K (9). Colourless gum; $[\alpha]^{25}_D$ +16.5 (*c* 0.10, MeOH); UV (MeOH) λ_{max} (log ε) 200 (2.82), 265 (0.85) nm; IR (KBr) v_{max} 3450, 1697, 1611, 1572, 1382, 1250 cm^{-1}; for ^{1}H and ^{13}C NMR data, see ESI Tables S1 and S2†; ESIMS (positive) *m/z* 661.7 [M+H]$^+$; HRESIMS *m/z* 683.3550 [M+Na]$^+$ (calcd for C$_{40}$H$_{52}$NaO$_8$, 683.3554).

Aphanamene L (10). Colourless gum; $[\alpha]^{25}_D$ −13.5 (*c* 0.10, MeOH); UV (MeOH) λ_{max} (log ε) 200 (2.92), 265 (0.89) nm; IR (KBr) v_{max} 3449, 1697, 1611, 1573, 1382, 1250 cm^{-1}; for ^{1}H NMR data, see ESI Tables S1†; ESIMS (positive) *m/z* 661.6 [M+H]$^+$; HRESIMS *m/z* 683.3550 [M+Na]$^+$ (calcd for C$_{40}$H$_{52}$NaO$_8$, 683.3554).

Aphanamene M (11). Colourless gum; $[\alpha]^{25}_D$ +16.2 (*c* 0.10, MeOH); UV (MeOH) λ_{max} (log ε) 200 (2.72), 265 (0.99) nm; IR (KBr) v_{max} 3450, 1697, 1611, 1573, 1382, 1250 cm^{-1}; for ^{1}H and ^{13}C NMR data, see ESI Tables S1 and S2†; ESIMS (positive) *m/z* 661.6 [M+H]$^+$; HRESIMS *m/z* 683.3556 [M+Na]$^+$ (calcd for C$_{40}$H$_{52}$NaO$_8$, 683.3554).

Aphanamene N (12). Colourless gum; $[\alpha]^{25}_D$ −6.0 (*c* 0.10, MeOH); UV (MeOH) λ_{max} (log ε) 200 (2.66), 265 (0.83) nm; IR (KBr) v_{max} 3455, 1699, 1613, 1574, 1384, 1252 cm^{-1}; for ^{1}H NMR data, see ESI Tables S1†; ESIMS (positive) *m/z* 661.6 [M+H]$^+$; HRESIMS *m/z* 683.3556 [M+Na]$^+$ (calcd for C$_{40}$H$_{52}$NaO$_8$, 683.3554).

Aphanamene O (13). Colourless gum; $[\alpha]^{25}_D$ +26.2 (*c* 0.12, MeOH); UV (MeOH) λ_{max} (log ε) 198 (2.34), 265 (0.39) nm; IR (KBr) v_{max} 3444, 1696, 1611, 1572, 1382, 1250 cm^{-1}; for ^{1}H and ^{13}C NMR data, see ESI Tables S1 and S2†; ESIMS (positive) *m/z* 661.7 [M+H]$^+$; HRESIMS *m/z* 683.3552 [M+Na]$^+$ (calcd for C$_{40}$H$_{52}$NaO$_8$, 683.3554).

Aphanamene P (14). Colourless gum; $[\alpha]^{25}_D$ −13.6 (*c* 0.10, MeOH); UV (MeOH) λ_{max} (log ε) 198 (2.29), 265 (0.30) nm; IR (KBr) v_{max} 3447, 1696, 1611, 1572, 1382, 1250 cm^{-1}; for ^{1}H NMR data, see ESI Tables S1†; ESIMS (positive) *m/z* 661.6 [M+H]$^+$; HRESIMS *m/z* 683.3552 [M+Na]$^+$ (calcd for C$_{40}$H$_{52}$NaO$_8$, 683.3554).

NO production bioassay

The macrophage cell line RAW264.7 was purchased from the Chinese Academic of Sciences. The cells were cultured in DMEM containing 10% FBS with penicillin (100 U/mL) and streptomycin (100 U/mL) at 37 ºC in a humidified atmosphere with 5% CO$_2$. The cells were allowed to grow in 96-well plates with 1×10^5 cells to treat test compounds. After incubated for 2 h, the cells were treated with 100 ng/mL of LPS for 18h. Nitrite in culture media was measured to assess NO production using Griess reagent. The absorbance at 540nm was measured on a microplate reader. N-monomethyl-L-arginine was used as the positive control. Cytotoxicity was determined by MTT method, after 48h incubation with test compounds. All the experiments were performed in three independent replicates.

Notes and references

State Key Laboratory of Natural Medicines, Department of Natural Medicinal Chemistry, China Pharmaceutical University, 24 Tong Jia Xiang, Nanjing 210009, People's Republic of China

Tel /Fax: +86-25-83271405

Email: luojun1981ly@163.com; cpu_lykong@126.com

† Electronic Supplementary Information (ESI) available: HRESIMS, CD, 1D and 2D NMR spectra for the compounds **1**−**14**, together with the ^{1}H, ^{13}C data and CD of **9**−**14** (Table S1 and S2, Fig. S1) and Scheme S1. See DOI: 10.1039/b000000x/

1. S.-K. Chen, B.-Y. Chen and H. Li, Flora Reipublicae Popularis Sinicae, Science Press, Beijing, 1997, **43**, p. 75-80.
2. E. committee., Chinese Materia Medica, Shanghai Science and Technology Publisher, Shanghai, 1999, **13**, p. 31.
3. J.-Y. Cai, Y. Zhang, S.-H. Luo, D.-Z. Chen, G.-H. Tang, C.-M. Yuan, Y.-T. Di, S.-H. Li, X.-J. Hao and H.-P. He, *Organic letters*, 2012, **14**, 2524-2527.
4. S.-P. Yang, H.-D. Chen, S.-G. Liao, B.-J. Xie, Z.-H. Miao and J.-M. Yue, *Organic letters*, 2010, **13**, 150-153.
5. Y. Zhang, J.-S. Wang, X.-B. Wang, D.-D. Wei, J.-G. Luo, J. Luo, M.-H. Yang and L.-Y. Kong, *Tetrahedron Letters*, 2011, **52**, 2590-2593.
6. Y. Zhang, J.-S. Wang, D.-D. Wei, Y.-C. Gu, X.-B. Wang and L.-Y. Kong, *J Nat Prod*, 2013, **76**, 1191-1195.
7. Y. Zhang, J.-S. Wang, D.-D. Wei, X.-B. Wang, J. Luo, J.-G. Luo and L.-Y. Kong, *Phytochemistry*, 2010, **71**, 2199-2204.
8. J.-S. Wang, Y. Zhang, X.-B. Wang, D.-D. Wei, J. Luo, J.-G. Luo, M.-H. Yang, H.-Q. Yao, H.-B. Sun and L.-Y. Kong, *Tetrahedron Letters*, 2012, **53**, 1705-1709.
9. Y. Zhang, J.-S. Wang, J. Luo and L.-Y. Kong, *Chemical and Pharmaceutical Bulletin*, 2011, **59**, 282-286.
10. H.-J. Zhang, J. Luo, S.-M. Shan, X.-B. Wang, J.-G. Luo, M.-H. Yang and L.-Y. Kong, *Organic letters*, 2013, **15**, 5512-5515.
11. J. Liu, X.-F. He, G.-H. Wang, E. F. Merino, S.-P. Yang, R.-X. Zhu, L.-S. Gan, H. Zhang, M. B. Cassera, H.-Y. Wang and J.-M. Yue, *The Journal of organic chemistry*, 2013, **79**, 599-607.
12. J.-P. Yin, M. Gu, Y. Li and F.-J. Nan, *The Journal of organic chemistry*, 2014, **79**, 6294-6301.
13. S. Chimichi, M. Boccalini, B. Cosimelli, F. Dall, G. Viola, D. Vedaldi and F. Dall'Acqua, *Tetrahedron Letters*, 2002, **43**, 7473–7476.
14. H.-Y. Zhang, C.-M. Yuan, M.-M. Cao, X.-H. Li, S.-L. Li, Y. Zhang, X.-J. Hao and H.-P. He, *Phytochemistry Letters*, 2014, **8**, 81-85.
15. R. Zhang, H.-P. He, Y.-T. Di, S.-L. Li, G.-Y. Zuo, Y. Zhang and X.-J. Hao, *Fitoterapia*, 2014, **92**, 100-104.

Organic & Biomolecular Chemistry Accepted Manuscript